

PAPER • OPEN ACCESS

Φ -OTDR based on tunable Yb-Er:phosphate-glass laser

To cite this article: T V Choban *et al* 2019 *J. Phys.: Conf. Ser.* **1410** 012108

View the [article online](#) for updates and enhancements.



IOP | ebooks™

Bringing together innovative digital publishing with leading authors from the global scientific community.

Start exploring the collection—download the first chapter of every title for free.

Φ -OTDR based on tunable Yb-Er:phosphate-glass laser

T V Choban¹, A A Zhirnov¹, A O Chernutsky¹, K V Stepanov¹, A B Pnirov¹,
G Galzerano², V E Karasik¹, C Svelto³

¹Bauman Moscow State Technical University, Moscow 105005, Russia

²IFN-CNR, Milano 20133, Italy

³DEIB, Politecnico di Milano, Milano 20133, Italy

Abstract. In recent times, phase-sensitive optical time domain reflectometers became widely common for monitoring of extended objects and providing necessary measurements in optical telecommunications. In this paper we present our investigations and results in the development and characterization of a new type of laser for phase-sensitive optical time domain reflectometry.

1. Introduction

Phase-sensitive optical time domain reflectometers (ϕ -OTDR) are widely used in remote monitoring systems, providing a great amount of measurements for plants installation and security (pipelines, railway tracks, perimeter security, etc.), in proximity of an optical fiber [1-5]. The most important component of a ϕ -OTDR is its laser source, which defines the quality of the system. Different requirements arise for a laser providing efficient and well-precise operation of the ϕ -OTDR. The Yb-Er:glass solid-state laser [6] presents a great interest as it has very good short-term wavelength stability and possibility of wavelength tuning for compensation of ϕ -OTDR sensitivity 'dead zones'. One significant question is about finding the most adequate structure of the laser system, achieving the accuracy requirements for ϕ -OTDR with a simple and practical minilaser setup.

2. Laser system for ϕ -OTDR

In previous works we have studied a microchip Yb-Er:glass laser, measuring amplitude and phase noise of this laser setup [7]. Its main problems were high RIN peak level and frequency, due to relaxation oscillations in the short and lossless laser cavity, and the complex wavelength/cavity tuning. Based on this experience, we modified the structure of the laser to solve these problems. Now the resonator is formed by a 1 mm-thick Yb-Er:glass gain medium and an external concave mirror. Pumped by a fiber-coupled semiconductor laser diode at 976 nm, this plane-spherical laser operates in the range 1532..1570 nm. The structure of the resonator is shown in Fig. 1: first surface of the gain medium reflects laser radiation and is transparent for the pump ($R_{1@1550\text{nm}} > 99.9\%$, $R_{1@976\text{nm}} < 2\%$); second surface of gain medium is transparent for laser radiation and reflects the pump ($R_{2@1550\text{nm}} < 0.02\%$, $R_{2@976\text{nm}} > 80\%$); concave mirror reflects laser radiation providing 0.5 % output coupling ($R_{3@1550\text{nm}} = 99.5\%$). Maximum cavity length is limited by the radius of curvature of the mirror (now $ROC = 50$ mm). A GaAs plate is an additional component that can be placed inside the resonator in order to provide better wavelength stability and RIN reduction.



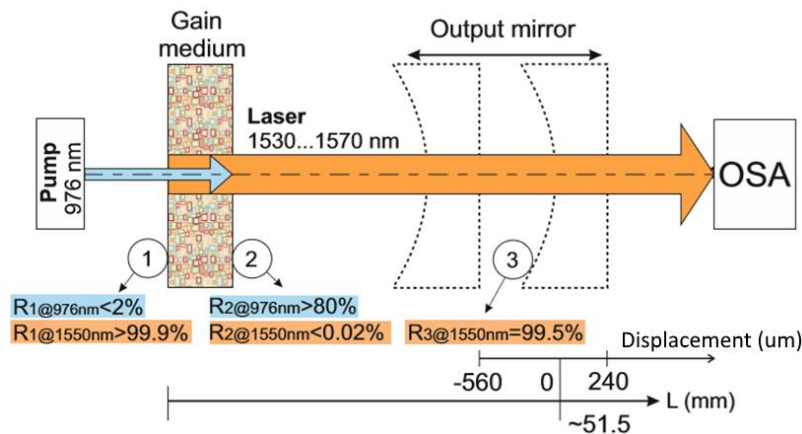


Figure 1. Structure of the laser resonator used in experiments and output mirror displacements.

Example of laser multi-longitudinal-mode output spectrum, depending on cavity length, is shown in Fig. 2. As the position of output mirror is changeable, we have experimentally studied how laser output spectrum depends on resonator construction in order to find the most adequate lengths of the resonator. One can see that the laser with maximum cavity length generates the widest output spectrum, which is important for wavelength tuning. Due to the spherical mirror, different cavity lengths provide laser beams with different waist diameters and thus working in different net gain conditions (gain in pumped region minus losses in unpumped regions minus other losses). Shorter cavity provides for larger waist diameter, which is shown in Fig. 3 (a), and in this case low population inversion zones appear within the laser mode volume. Fig. 3 (b) shows the gain spectrum of Er^{3+} . One can see that large waist diameter beams create reabsorption losses at 1535 nm in unpumped regions of active medium and thus generation in region 1540..1565 nm becomes more probable.

One of the emitted wavelengths is chosen by an optical band-pass filter. By coarsely and finely adjusting laser cavity length, it is possible to provide laser wavelength tuning which is important for matching with optical filter in ϕ -OTDR scheme.

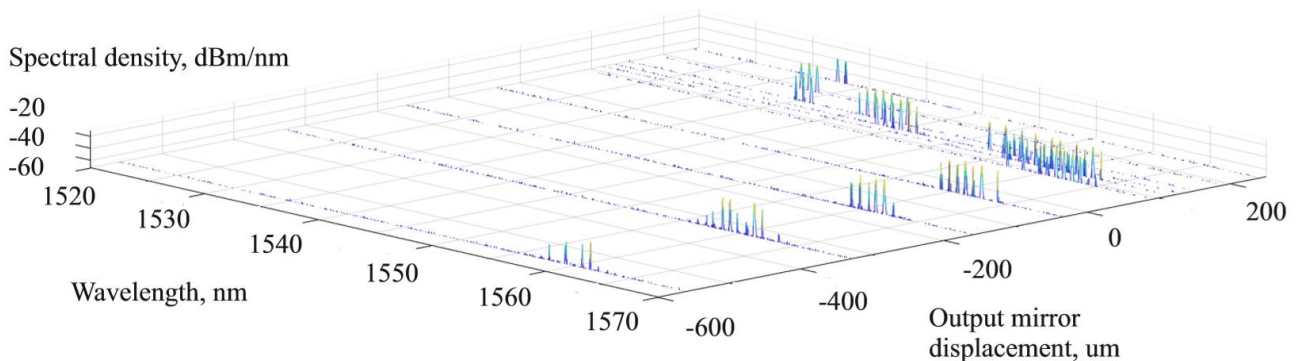


Figure 2. Multi-longitudinal-mode output spectrum of the laser depending on cavity length.

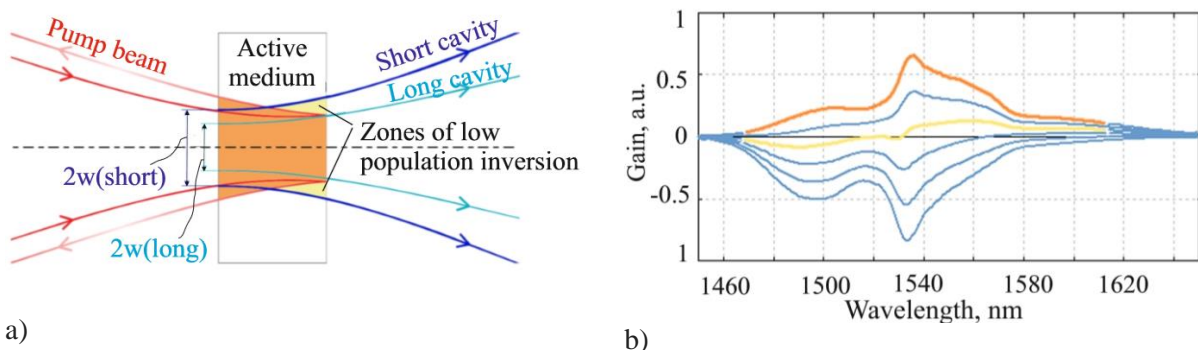


Figure 3 (a, b). a) Population inversion in Er-Yb:glass active medium; b) Er^{3+} gain spectrum. Yellow refers to low population inversion and orange refers to high population inversion.

While developing a laser for ϕ -OTDR, the most important requirements are wavelength and amplitude stability. In order to decrease the amplitude of relaxation oscillations, we used a two-photon absorber GaAs plate inside of the resonator, as GaAs energy levels configuration allows for laser output power stabilization. RIN peak frequency in this system (Fig. 4 (a)) decreased compared to the microchip laser [7] due to the now much longer cavity. Fig. 4 (b, c) show frequency deviations of microchip laser and plane-spherical laser respectively. Reducing amplitude of relaxation oscillations leads to significant increase of Signal-to-Noise Ratio (SNR), providing for better ϕ -OTDR operation.

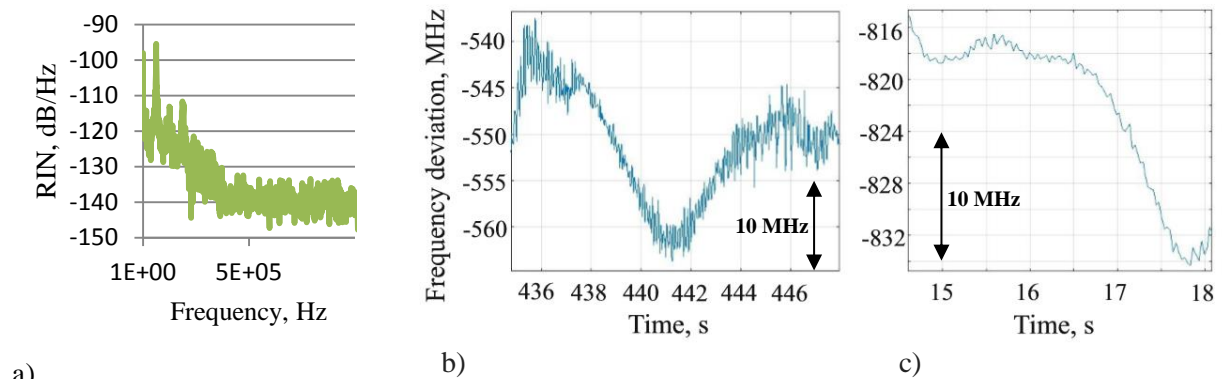


Figure 4 (a, b, c). a) Plane-spherical laser RIN spectrum; b) Microchip laser frequency deviations; c) Plane-spherical laser frequency deviations.

3. Φ -OTDR experimental scheme

The newly developed plane-spherical Yb-Er:glass laser was embedded in ϕ -OTDR experimental system, which is shown in Fig. 5 (a), quite different from common ϕ -OTDR scheme [8]. Light beam, emitted by the laser system is coupled into optical fiber (1). Optical circulator (2) delivers the light to a tunable filter (3), which we used for choosing just one longitudinal mode in (2)→(4) light propagation, as well as for suppressing ASE noise of the optical preamplifier (10) in (4)→(2) light propagation. Due to optical circulator (4) light is amplified by EDFA-booster (5) and is modulated by AOM (6). Passing through the third optical circulator (7), a light pulse goes to a sensing fiber (8). Propagating through sensing fiber, the light pulse is scattered on refractive index inhomogeneities. Back-scattered light returns to the system, so optical circulator (7) delivers it to EDFA-preamplifier (10). As mentioned earlier, light passes again through filter (3) and is detected by photoreceiver (11), being then processed by ADC (12) and personal computer (13). To observe output signal changes in time, we influenced the sensing fiber (8) with a PZT actuator (9). The PZT is a cylinder with 20 m of fiber coiled on it. We performed experiments with sine-wave electrical signal driving the PZT, with different frequencies: 10, 30, 50 and 70 Hz – most typical for real signals – and amplitude 3 V. In Fig. 5 (b) one can see how ϕ -OTDR output intensity changes with and without operating PZT (at 70 Hz), which is emulating a disturbance to the monitored structure along which the sensing fiber is buried. In plot of standard deviation (orange line) the region of PZT work can be easily distinguished.

Fig. 6 (a) shows an obtained reflectogram sequence (“waterfall”), having good visibility and sharpness, as obtained by novel plane-spherical laser. For comparison, in Fig. 6 (b) is presented waterfall obtained by previous laser with not enough wavelength stability.

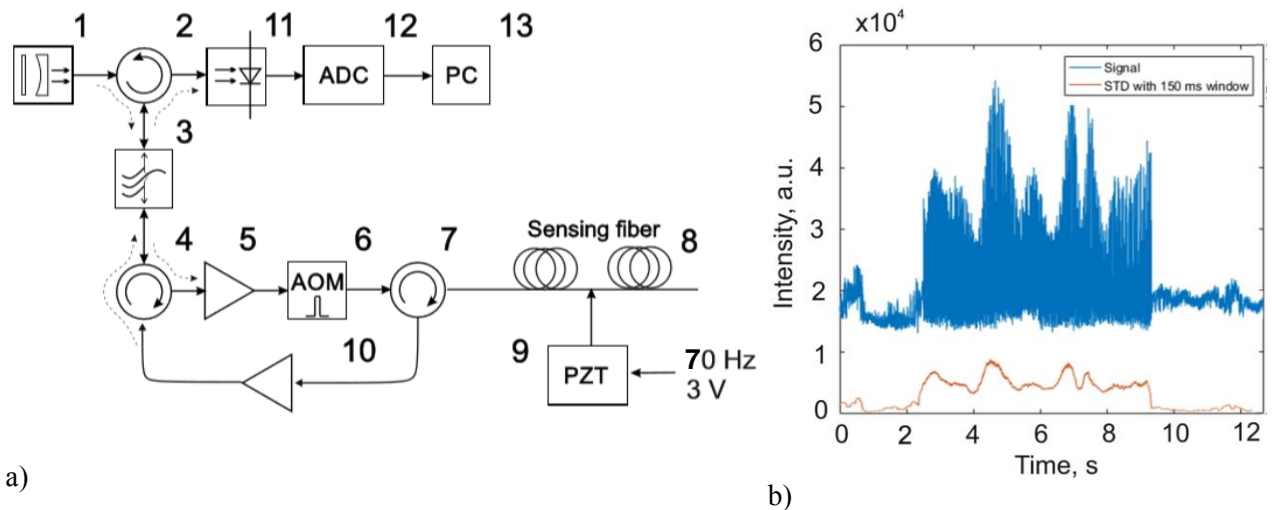


Figure 5 (a, b). **a)** Experimental scheme of ϕ -OTDR. 1 – laser; 2, 4, 7 – optical circulator; 3 – tunable filter; 5 – EDFA-booster; 6 – Acousto-Optic Modulator; 8 – sensing fiber; 9 – PZT actuator; 10 – EDFA-preamplifier; 11 – photoreceiver; 12 – ADC; 13 – personal computer; **b)** Intensity of an output signal in time with operating PZT from 2.51 s to 9.34 s.

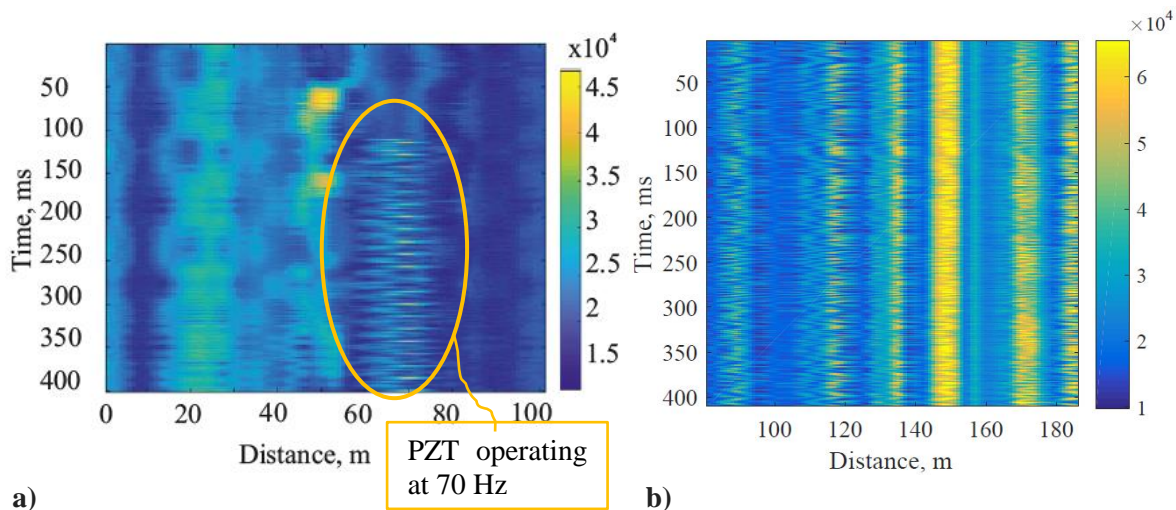


Figure 6 (a, b). Obtained ϕ -OTDR “waterfall”: start point in time ($t=0$ ms) is equivalent to the stimulus start ($t=2.51$ s) in Fig. 5 (b). Output intensity is shown with colours. **(a)** “Waterfall” from laser with enough wavelength stability. **(b)** Waterfall from laser with not enough wavelength stability.

To assess ϕ -OTDR performance, we estimated SNR as the ratio of signal standard deviation to noise standard deviation:

$$SNR = 20 \log \left(\frac{STD_S}{STD_N} \right)$$

We have observed output signal changing in time under 10, 30, 50 and 70 Hz influence, emulating a disturbance to the monitored structure. For each frequency we choose regions with duration 2 s under PZT operating (e.g. from 4 to 6 s in Fig. 5 (b)) and calculated standard deviation STD_S during this time interval, which refers to signal (with actually added noise) standard deviation. For STD_N calculations we choose a 2 s time interval from the same sensor point without PZT operating, so standard deviation calculated in this interval referred to just-noise standard deviation in each of the

experiments for the four frequencies of the influence signals. Results for different frequencies are given in Table 1.

Table 1. SNR for different external influences (corresponding to different PZT frequencies).

Frequency, Hz	SNR, dB
10	12.6
30	12.2
50	15.6
70	17.8

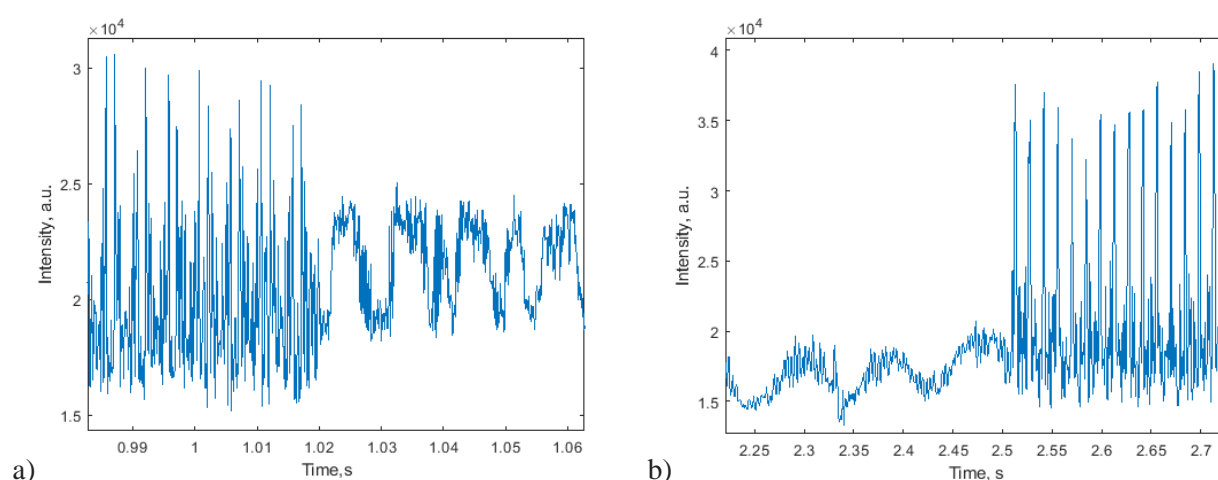


Figure 7 (a, b). (a) Signal with oscillations from impact at 10 Hz (before 1.02 s) and just from laser frequency instability (after 1.02 s); (b) Signal with oscillations from impact at 70 Hz (after 2.5 s) and just from laser frequency instability (before 2.5 s).

Fig. 7 (a) shows two regions of signal instability: due to PZT disturbance in left part and due to laser frequency fluctuations in right part. Besides, Fig. 7(b) clearly shows that laser frequency fluctuations have a shape corresponding to some sine-wave disturbance. It is worth noting that oscillations (due to mechanical vibrations) in the laser wavelength deviations lead to output signal fluctuations, causing SNR decrease. The way to solve this problem is to rigidly connect the resonator components, reducing such oscillations. Our further investigations are aimed to develop a monolithic cavity and first step will be creation of glued connection between active medium and GaAs plate. This will allow to avoid additional vibrations from plate and decrease RIN level due to its two photon absorption [9].

4. Conclusion

In this paper we proposed a structure of an Yb-Er:glass laser system for ϕ -OTDR, meeting the requirements of high enough stability operation. An adjustable cavity length allows for wavelength tuning, so we reported about the most adequate structure of the resonator by choosing proper cavity length. An experimental setup of ϕ -OTDR was assembled with the plane-spherical laser embedded. The proposed scheme provided for reflectogram sequences with good visibility and sharpness, which confirms suitable operation of this ϕ -OTDR system using the erbium minilaser.

Acknowledgments

The reported study was funded by RFBR according to the research project № 18-32-00688.

References

- [1] Honglan L, Zhenhai Z, Fei J 2018 Int. Conf. on Optical Instruments and Technology: Advanced Optical Sensors and Applications (Beijing) vol 10618 (SPIE-Intl Soc Optical Eng) 1061804
- [2] Ölçer İ, Öncü A 2018 Fiber Optic Sensors and Applications XV (Orlando) vol 10654 (SPIE) 106540C
- [3] Alekseev A E, Gorshkov B G, Potapov V T 2019 *Laser Phys.* 29(5) 055106
- [4] Nesterov E T, Treshchikov V N, Ozerov A Z, Sleptsov M A, Kamynin V A, Nanii O E and Sus'yan A A 2011 *Technical Physics Letters* 37(5) 417-420
- [5] Hartog A, Liokumovich L B, Ushakov N A, Kotov O I, Dean T, Cuny T and Constantinou A 2018 *Geophysical Prospecting* 66(S1) 192-202
- [6] Taccheo S, Laporta P, Longhi S, Svelto O, Svelto C 1996 *Applied Phys. B Laser and Optics* 63 (5) 425–436
- [7] Pniou A, Zhirnov A, Shelestov D, Stepanov K, Nesterov E, Karasik V, Laporta P, Galzerano G, Taccheo S, Piroddi L, Norgia M, Pesatori A, Svelto C 2016 *ACTA IMEKO* 5 (4) 24–28
- [8] Zhirnov A A, Pnev A B, Svelto C, Norgia M, Pesatori A, Galzerano G, Laporta P, Shelestov D A, Karasik V E 2017 *J. Phys.: Conf. Ser.* 917 052032
- [9] Van Leeuwen R, Xu B, Watkins L S, Wang Q, Ghosh C 2008 Enabling Photonics Technologies for Defense, Security, and Aerospace Applications IV (Orlando) vol 6975 (SPIE) 69750K